RSC Advances


This is an *Accepted Manuscript*, which has been through the Royal Society of Chemistry peer review process and has been accepted for publication.

*Accepted Manuscripts* are published online shortly after acceptance, before technical editing, formatting and proof reading. Using this free service, authors can make their results available to the community, in citable form, before we publish the edited article. This *Accepted Manuscript* will be replaced by the edited, formatted and paginated article as soon as this is available.

You can find more information about *Accepted Manuscripts* in the Information for Authors.

Please note that technical editing may introduce minor changes to the text and/or graphics, which may alter content. The journal's standard Terms & Conditions and the Ethical guidelines still apply. In no event shall the Royal Society of Chemistry be held responsible for any errors or omissions in this *Accepted Manuscript* or any consequences arising from the use of any information it contains.

ROYAL SOCIETY OF CHEMISTRY

www.rsc.org/advances

Journal Name

RSCPublishing

COMMUNICATION

# Highly conductive polymer composites incorporated with electrochemically exfoliated graphene fillers†

Cite this: DOI: 10.1039/x0xx00000x

Seung Han Ryu, Seil Kim, Han Kim, Sung-Oong Kang,* and Yong-Ho Choa*

Received 00th January 2014,
Accepted 00th January 2014

DOI: 10.1039/x0xx00000x

www.rsc.org/

**Highly conductive polymer composites were fabricated with a novel type of graphene-based filler, electrochemically exfoliated graphene sheets (EGs) produced without conventional oxidation/reduction of graphene oxide (GO). The high electrical conductivity of 417 ± 83 S/m at a content loading of 5.8 vol.% and a low percolation threshold of 0.37 vol.% could be attainable. Microscopic and spectroscopic investigations demonstrated the effective dispersion of EG-fillers on the surface of polymer particles and visualized the actual conducting channel between the polymer matrices.**

Polymer composite materials with enhanced electrical and mechanical properties have been explored upon synergetic effects of their comprising components, which are usually incorporated with a functional second-phase filler into polymer matrices.[1-3] In particular, conductive polymer composites are considered to be a key material in electronic devices, actuators, sensors and electromagnetic interference shielding.[4-7] As a promising filler in the conductive polymer composites, graphene, a single atomic layer of two-dimensional and conjugated carbon network, has recently stood in the spotlight due to its specific geometric features of large surface area and high aspect ratio in addition to its exceptional electrical, thermal and mechanical properties.[3,8-19] In order for industrial implementation of graphene-based conductive polymer composites, bulk-quantity production of graphene should be first addressed while maintaining the excellent intrinsic electrical properties.

Despite conspicuous high-quality of graphene nanosheets fabricated *via* mechanical exfoliation, epitaxial growth and chemical vapour deposition,[20-22] the high-temperature process, use of a sacrificial metal and multistep processing steps have substantially impeded these production routes to be used for the massive graphene production. In alternative, a solution-process based on chemical exfoliation of graphite into graphene oxide (GO) and the following reduction of GO into reduced GO (rGO) has opened a cost-effective way to the bulk-production of graphene.[23-26] However, the chemical oxidation of graphite into GO inevitably results in covalent modification of aromatic carbon networks with various oxygen-containing groups such that significantly damage the crystalline layers of graphene, which degrades the unique properties of individual graphene sheets. Furthermore, the reduction process is prone to irreversibly aggregate rGO sheets that disturb homogeneous dispersion and incorporation of graphene fillers into the polymer matrices. Nevertheless, graphene-based polymer composites mainly have employed the rGO-based fillers reduced from GO.[3,9-19]

The trade-off between the production scale and the quality of graphene fillers can be compromised by a electrochemical exfoliation approach, which enables the massive production of high-quality graphene sheets due to its simple, high-yield and environmentally benign process.[27-29] In the electrochemical exfoliation system, the gas species are evolved from electrochemical-potential-assisted oxidation of electrolyte at the edges and subsurface of graphite layers and induces the vertical and horizontal expansion and exfoliation of graphite layers into graphene sheets. As a result, the large-scale production of high-quality electrochemically exfoliated graphene sheets (EGs) provide a novel type of conducting fillers for highly conductive polymer composites.

Motivated by the attracting features of EGs, here, we incorporated the EG fillers into poly(methyl methacrylate) (PMMA) polymer matrices, which is a versatile polymer with the advantages of low price, optical transparency and mechanical strength.[30,31] Without the conventional oxidation/reduction process to prepare the graphene-based fillers, the EGs/PMMA polymer composites showed the high electrical conductivity of 417 ± 83 S/m at a content loading of 5.8 vol.%. The electrical transition of insulator-to-conductor was measured to occur at the low percolation threshold of 0.37 vol.%. The critical exponent fitted by a scaling law indicates the electrical conduction of EGs/PMMA composites through 3-dimensional (3D) conducting EG-filler networks between the polymer matrices. Microscopic and spectroscopic investigations could demonstrate the effective dispersion of EG-fillers on the surface of polymer particles

RSC Advances Accepted Manuscript

and visualized the actual conducting channel width to be a critical geometric parameter to explain the percolation behaviour.

EGs were electrochemically exfoliated in an aqueous solution of inorganic salt (ammonium sulfate, $(NH_4)_2{\cdot}SO_4$)).[29] A typical exfoliation process was carried out in a two electrode system containing the 0.1 M electrolyte solution where graphite foil (Alfa Aesar) and Pt foil used as anode and cathode, respectively. The positive DC potential applied to the anode was fixed to be 10 V. The as-obtained EGs were collected by vacuum filtration through an anodized aluminum oxide (AAO) membrane and rinsed with distilled water several times. Thin EGs could be obtained *via* dispersion of product into dimethylformamide (DMF) solvent using bath sonication for 10 min and a centrifuge at 4000 rpm for 10 min. After being centrifuged, the sediment of dispersion was decanted and the supernatant dispersion were collected, and used to fabricate the polymer composite. The final concentration of EG-dispersion was controlled to be 1 mg/ml.

Morphology and thickness of EGs were characterized by atomic force microscopy (AFM). Figure 1a presents a typical AFM image of EGs loaded onto a $SiO_2$ substrate using the Langmuir−Blodgett technique.[32] Most of EGs were measured to have lateral sizes in a range of 1 – 5 $\mu$m. A statistical profiling from the AFM height measurements of 100 EGs discloses that 65% of EGs are thinner than 6-layer of graphene (Fig. S1 in the ESI†). The thickness of EGs could be roughly averaged to 5.02 nm (± 2.06 nm). TEM image in Fig. 1b displays a few-layered EGs with the lateral size of approximately 3 $\mu$m consistent with those of EGs measured by the AFM technique. The selected area electron diffraction (SAED) pattern of EG shows the 6-fold symmetry of hexagonal crystalline structure (the inset of Fig. 1b). Chemical structure and composition of EGs was probed using X-ray photoelectron spectroscopy (XPS). The deconvolution of C1s XPS peak (Fig. 1c) represents four carbon atomic components assigned to C-C (284.5 eV), C-O (286.3 eV), C=O (289.1 eV) and O-C=O (289.1 eV).[33] The oxygen-functional groups on the basal and edges of graphene sheets has been reported to originate from the over-oxidation unavoidable during the electrochemical process.[27,28] However, the carbon to oxygen ratio (C/O ratio) of the as-prepared EGs was measured to be 10.34, importantly, without the post-reduction step.

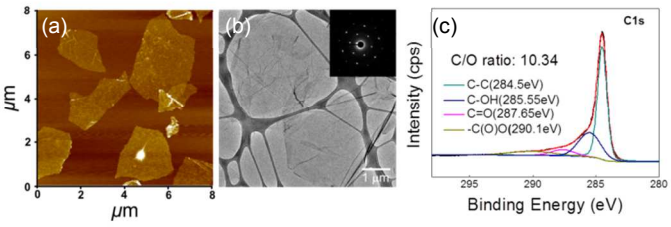


Fig. 1. Morphology, thickness and chemical structure of EGs characterized using (a) AFM, (b) TEM and (c) XPS.

In order to investigate the electrical property of EGs, a free-standing EG film was fabricated through vacuum filtration and vacuum drying at 200°C. The electrical conductivity of EG films was measured to be $2.12 \times 10^4$ S/m using a 4-probe system. Here, it needs to be pointed out that the C/O ratio and the electrical conductivity of EGs are comparable with those of highly reduced rGO using a hydrohalic (HI) acid, which recently has been used to fabricate 3D interconnected graphene networks in highly conductive rGO/polystyrene (PS) composites.[16,34]

To fabricate the segregated networks of EG-fillers, the controlled volume of EG-dispersion was first mixed with PMMA particles with a radius of 20 $\mu$m in DMF by stirring for 2 h. The EG-coated PMMA particles were precipitated and the supernatant transparent DMF solvent were decanted. The mixture was vacuum-filtrated, transferred into a vacuum oven and dried to a powder. Finally, the as-prepared powder was hot-pressed at 200 °C into a pellet with a radius of 25 mm and thickness of 1 mm. The fabrication steps for the EGs/PMMA composites with the segregated networks of EGs are schematically drawn in Fig. 2.

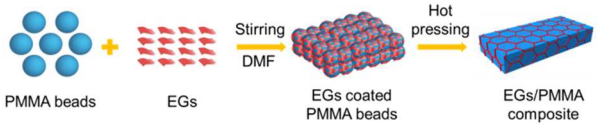


Fig. 2. Schematic illustration of EGs/PMMA composites with the segregated networks of EG-fillers.

Encapsulation of PMMA polymer particles with the EGs-fillers could be observed by scanning electron microscopy (SEM). In comparison with the bare surfaces of PMMA particles (Fig. 3a), the shagged surface of EGs/PMMA particle depicts the entire coating of EGs over the surface of PMMA particle (Fig. 3b). The following hot-press step localizes the fillers of EGs at the boundaries between the polymer particles and further form the continuous conducting regions or channels of EGs with the segregated distribution inside the insulating polymer matrices. As recognized in SEM images of Fig. 3c and d, the hot-pressed polyhedrons are covered with the overlapped and compacted multilayers of EGs. The layer of EGs stacked on the surface of PMMA particles were further confirmed by Raman spectroscopy. The Raman spectrum of EGs/PMMA particle (Fig. S2 in the ESI†) shows a prominent G peak at ~1575 $cm^{-1}$ from the first-order scattering of E2g vibrational mode of $sp^2$ carbon atoms associated with the degree of graphitization. On the other hand, the D band is observed at ~1350 $cm^{-1}$ related to the breathing mode of $sp^3$ carbon atoms from the structural defects and partially disordered structures, such as edges and oxygen-functional groups.[35] It was also seen that the graphene sheets exhibited a broad and up-shifted 2D band at around 2700 $cm^{-1}$, which indicates a few-layered EGs. The ratio between the intensity of G and D peaks ($I_D/I_G$) was calculated to be 0.58 that is much lower than those of chemically or thermally reduced rGO indicates the high-quality of EGs.[25,35,36]

RSC Advances Accepted Manuscript


This journal is © The Royal Society of Chemistry 2014

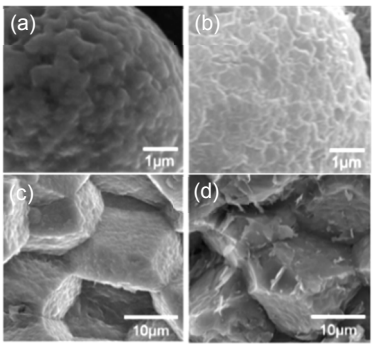


Fig. 3. SEM observation of (a) the bare- and (b) the EG-encapsulated of unpressed PMMA particles, and (c) the bare- and (d) the EG-coated PMMA polyhedrons.

The direct current electrical conductivity of graphene/PMMA composites as a function of graphene volume fraction is shown in Fig. 4. According to the classical percolation theory, the electrical conductivity of the composites above the percolation threshold ($\varphi_c$) depends on the volume fraction of filler described by a scaling law:[37]

$$\sigma = \sigma_o(\varphi - \varphi_c)^t$$

where $\sigma$ is the electrical conductivity of composite, $\sigma_o$ the electrical conductivity of filler, $\varphi$ the volume fraction of filler, $\varphi_c$ the percolation threshold and $t$ is a critical exponent. At a percolation threshold, the fillers construct the interconnected networks of conducting paths throughout the insulating polymer matrices and thus induce a transition of insulator-to-conductor with a steep increase of electrical current of composites. The percolation in the EGs/PMMA composites was measured to occur at the filler concentration ($\varphi_c$) of 0.37 vol.%. Above the percolation threshold, the electrical conductivity of composites rapidly rises up to 112 ± 62 S/m at the filler loading of 2.2 vol.% and finally reaches 417 ± 83 S/m at 5.8 vol.%, which is notably higher than those of previous rGO-based polymer composites.[9-15] All values of percolation threshold and the electrical conductivity were averaged from five different samples. Plotting $\sigma$ vs ($\varphi - \varphi_c$) in double logarithmic coordinates results in the conductivity exponent ($t$) of 1.899 (the inset of Fig. 4), which relies on the dimensionality of composites. In a single percolation system, the calculated $t$ value in range of 1.6 – 2 stands for the formation of 3-dimensional conductive networks, in which the electrons transport through the interfaces between the polymer matrices.[37,38]

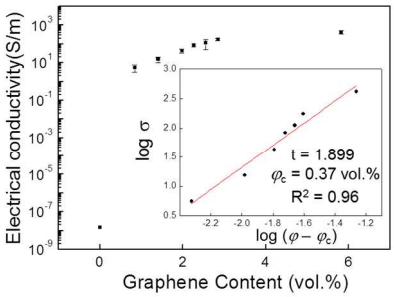


Fig. 4. Semi-log plot of electrical conductivity of the EGs/PMMA composites as a function of EG-filler content. The inset is a double-logarithmic plot of volume electrical conductivity $\sigma$ versus ($\varphi$-$\varphi_c$) with the fitted parameter of $t$ = 1.899, $\varphi_c$ = 0.37 vol. %.

In the segregated structure, the percolation behaviour parameterized by the percolation threshold ($\varphi_c$) and the critical exponent ($t$) primarily depends on dimensionality of fillers (the particle size, shape and aspect ratio) and the width of conducting channels filled with the fillers.[39,40] The channel width of conducting EG filler in the hot-pressed EGs/PMMA composites was observed using a cross-sectional transmission electron microscopy (TEM) technique. The cross-sectional TEM image visualizes the graphene fillers with the actual conducting channel width of ~23 nm between the PMMA polymer particles (Fig. S3 in the ESI†).

The percolation threshold has been believed to be a complex function of the dimension, shape, size, local variation in concentration and spatial distribution of fillers. To be specific, the percolation model on the segregated composite structure suggested that the percolation threshold substantially depends on the particle size ratio and the conducting channel width of fillers.[39,40] It seems reasonable that the thinner graphene fillers with the large lateral diameters are readily to build the specific conductive networks at a lower content loading than those made of thicker fillers. That is, the width of conducting channel localized between the polymer matrices is expected to be thinner, leading to the lower percolation threshold in the graphene/polymer composites. Such a relationship between the geometric factor and the percolation behaviour may be intuited by comparing the results of EGs/PMMA composites with those of rGO/PS and rGO/PMMA composites incorporated with 3D interconnected networks of HI-reduced and hydrazine ($N_2H_4$)-reduced rGO.[16,17] Despite the compatible oxidation degree and the electrical conductivity of EG fillers with those of the HI-reduced and the $N_2H_4$-reduced rGO fillers, the rGO/PS and the rGO/PMMA composites exhibited the relatively lower percolation threshold of 0.15 vol.% and 0.16 vol.%, respectively. It is understood that the thin rGO fillers made of mono- and few-layered sheets readily form the relatively narrower channel than the EG-based channels with the average thickness of 5.02 nm (±2.06 nm). In addition, the interaction between the fillers and the polymer matrices seems to affect the formation of conductive channel. For instance, the rGO/PS and the rGO/PMMA composites were designed upon self-assembling of the fillers and the surface-modified polymer particles with the opposite surface charges supposed to induce the strong and effective

RSC Advances Accepted Manuscript

adsorption of rGO sheets onto the surface of PS and PMMA particles.[16,17] In contrary, both surfaces of EGs and the PMMA particles were measured to be negatively charged with a zeta potential of -32 mV and -15 mV, respectively. The differenct surface charges of PMMA particles used in this work and the rGO/PMMA composite may be explained by different acceptor number of the solvent dimethylformamide (DMF) and deionized water.[41] The repulsive electrostatic interaction between EGs and the PMMA particles may play a role in the formation of the thicker conducting channel of loosely packed EGs, which may be just physically stacked during the drying process. As a result, the relatively higher percolation threshold and the lower electrical conductivity of EGs/PMMA composites could be achieved in comparison with those of rGO/PS and rGO/PMMA composite. Nevertheless, we believe that the approach of this work without the conventional oxidation/reduction steps of rGO would contribute to development of the highly conductive graphene-based polymer composites. The more systematic study on the relationship between the percolation behaviour and the geometric and electrical parameters is in progress.

In summary, a novel type of EG-fillers, which were electrochemically produced without the conventional oxidation/reduction steps of rGO, could be effectively incorporated into the highly conductive EG/sPMMA polymer composites. Microscopic and spectroscopic observations demonstrated the construction of 3D conducting EG-filler networks in the segregated structure between the polymer matrices. The as-fabricated EGs/PMMA composites exhibited the high electrical conductivity of 417 ± 83 S/m at a filler content of 5.8 vol.%. and the low percolation threshold of 0.37 vol.%.

## Acknowledgements

This work was supported by a grant from the Fundamental R&D Program for Core Technology of Materials(10050890, Chalcogenide nanostructure-based room-temperature (25°C) $H_2$ & $H_2S$ gas sensors with low power consumption) and under grant number 10047876 funded by the Ministry of Trade, Industry & Energy, Republic of Korea

## Notes and references

*Department of Fusion Chemical Engineering, Hanyang University, Ansan 426-791, Republic of Korea*
*E-mail: choa15@hanyang.ac.kr*

† Electronic supplementary information (ESI) available: Statistical thickness distribution of EGs using AFM measurement, Raman spectrum of EGs/PMMA particles and Cross-sectional TEM images. See DOI: 10.1039/b000000x/

1 K. Y. Chun, Y. Oh, J. Rho, J.-H. Ahn, Y.-J. Kim, H. R. Choi, S. Baik, *Nature Nanotechnology*, 2010, **5**, 853.
2 T. S. Hansen, K. West, O. Hassager, N. B. Larsen, *Adv. Funct. Mater.*, 2007, **17**, 3069.
3 S. Stankovich, D. A. Dikin, G. H. B. Dommett, K. M. Kohlhaas, E. J. Zimney, E. A. Stach, R. D. Piner, S. T. Nguyen, R. S. Ruoff, *Nature*, 2006, **442**, 282.
4 K. S. Kim, Y. Zhao, H. Jang, S. Y. Lee, J. M. Kim, K. S. Kim, J.-H. Ahn, P. Kim, J.-Y. Choi, B. H. Hong, *Nature*, 2009, **457**, 706.
5 Y. Hu, W. Chen, L. Lu, J. Liu, C. Chang, *ACS Nano*, 2010, **4**, 3498.
6 B. Y. Lee, K. Heo, J. H. Bak, S. U. Cho, S. Moon, Y. D. Park, S. Hong, *Nano Letters*, 2008, **8**, 4483.
7 J. Liang, Y. Wang, Y. Huang, Y. Ma, Z. Liu, J. Cai, C. Zhang, H. Gao, Y. Chen, *Carbon*, 2009, **47**, 922.
8. Y. Zhu, S. Murali, W. Cai, X. Li, J. W. Suk, J. R. Potts, R. S. Ruoff, *Adv. Mater.*, 2010, **22**, 3906.
9 J. R. Potts, D. R. Dreyer, C. W. Bielawski, R. S. Ruoff, *Polymer*, 2011, **52**, 5.
10 H. Kim, A. A. Abdala, C. W. Macosko, *Macromolecules*, 2010, **43**, 6515.
11 M.-C. Hsiao, S.-H. Liao, Y.-F. Lin, C.-A. Wang, N.-W. Pu, H.-M. Tsai, C.-C. M. Ma, *Nanoscale*, 2011, **3**, 1516.
12 J. Du, L. Zhao, Y. Zeng, L. Zhang, F. Li, P. Liu, C. Liu, *Carbon*, 2011, **49**, 1094.
13 H. Hu, G. Zhang, L. Xiao, H. Wang, Q. Zhang, Z. Zhao, *Carbon*, 2012, **50**, 4596.
14 M. Yoonessi, J. R. Gaier, *ACS Nano*, 2010, **4**, 7211.
15 M. Li, C. Gao, H. Hu, Z. Zhao, *Carbon*, 2013, **65**, 371.
16 C. Wu, X. Huang, G. Wang, L. Lv, G. Chen, G. Li, P. Jiang, *Adv Funct Mater*, 2013, **23**, 506.
17 V. H. Pham, T. T. Dang, S. H. Hur, E. J. Kim, J. S. Chung, *ACS Appl. Mater. Interfaces*, 2012, **4**, 2630.
18 Y.-T. Liu, M. Dang, X.-M. Xie, Z.-F. Wang, X.-Y. Ye, *J. Mater. Chem*, 2011, **21**, 18723.
19 Y.-T. Liu, X.-M. Xie, X.-Y. Ye, *Carbon*, 2011, **49**, 3529.
20 17 K. S. Novoselov, A. K. Geim, S. V. Morozov, D. Jiang, Y. Zhang, S. V. Dubonos, I. V. Grigorieva, A. A. Firsov, *Science*, 2004, **306**, 666.
21 C. Berger, Z. Song, X. Li, X. Wu, N. Brown, C. Naud, D. Mayou, T. Li, J. Hass, A. N. Marchenkov, E. H. Conrad, P. N. First,W. A. de Heer, *Science*, 2006, **312**, 1191.
22 Y. Lee, S. Bae, H. Jang, S. Jang, S.-E. Zhu, S. H. Sim, Y. I. Song, B. H. Hong, J.-H. Ahn, *Nano Letters*, 2010, **10**, 490.
23 W. S. Hummers, Jr., R. E. Offeman, *J. Am. Chem. Soc.*, 1958, **80** , 1339.
24 D. C. Marcano, D. V. Kosynkin, J. M. Berlin, A. Sinitskii, Z. Sun, A. Slesarev, L. B. Alemany, W. Lu, J. M. Tour, *ACS Nano*, 2010, **4**, 4806.
25 S. Stankovich, D. A. Dikin, R. D. Piner, K. A. Kohlhaas, A. Kleinhammes, Y. Jia, Y. Wu, S. T. Nguyen, R. S. Ruoff, *Carbon*, 2007, **45**, 1558.
26 D. R. Dreyer, S. Park, C. W. Bielawski, R. S. Ruoff, *Chem. Soc. Rev.*, 2010, **39**, 228.
27 C.-Y. Su, A.-Y. Lu, Y. Xu, F.-R. Chen, A. N. Khlobystov, L.-J. Li, *ACS Nano*, 2011, **5**, 2332.
28 K. Parvez, R. Li, S. R. Puniredd, Y. Hernandez, F. Hinkel, S. Wang, X. Feng, K. Müllen, *ACS Nano*, 2013, **7**, 3598.
29 K. Parvez, Z.-S. Wu, R. Li, X. Liu, R. Graf, X. Feng, K. Müllen, *J. Am. Chem. Soc.*, 2014, **136**, 6083.
30 G. Chen, J.H. Li, S. Qu, D. Chen, P.Y. Yang, *J. Chromatogr. A* 2005, **1094**, 138.

RSC Advances Accepted Manuscript

 This journal is © The Royal Society of Chemistry 2014

31 G.X. Xu, J. Wang, Y. Chen, L.Y. Zhang, D.R. Wang, G. Chen, *Lab Chip* 2006, **6**, 145.
32 27 X. Li, G. Zhang, X. Bai, X. Sun, X. Wang, E. Wang, H. Dai, *Nature Nanotechnology*, 2008, **3**, 538.
33 M. J. McAllister, J.-L. Li, D. H. Adamson, H. C. Schniepp, A. A. Abdala, J. Liu, M. H.-Alonso, D. L. Milius, R. Car, R. K. Prud'homme, I. A. Aksay, *Chem. Mater.*, 2007, **19**, 4396.
34 S. Pei, J. Zhao, J. Du, W. Ren, H.-M. Cheng, *Carbon*, 2010, **48**, 4466.
35 C. Mattevi, G. Eda, S. Agnoli, S. Miller, K. A. Mkhoyan, O. Celik, D. Mastrogiovanni, G. Granozzi, E. Garfunkel, M. Chhowalla, *Adv. Funct. Mater.*, 2009, **19**, 2577.
36 V. López, R. S. Sundaram, C. G.-Navarro, D. Olea, M. Burghard, J. G.-Herrero, F. Zamora, K. Kern, *Adv. Mater.*, 2009, **21**, 4683.
37 D. Stauffer, A. Aharony, *Introduction To Percolation Theory*, Taylor and francis, London, 1994.
38 J. F. Gao, Z. M. Li, Q. J. Meng, Q. Yang, *Mater. Lett*. 2008, **62**, 3530.
39 M. O. Lisunova, Ye. P. Mamunya, N. I. Lebovka, A. V. Melezhyk, *European Polymer Journal*, 2007, **43**, 949.
40 Ye. Mamunya, A. Boudenne, N. Lebovka, L. Ibos, Y. Candau, M. Lisunova, *Composites Science and Technology*, 2008, **68**, 1981.
41 W. W. Liu, J. N. Wang, X. X. Wang, *Nanoscale*, 2012, **4**, 425.

RSC Advances Accepted Manuscript